

Published in final edited form as:

Science. 2012 August 24; 337(6097): 980–984. doi:10.1126/science.1224896.

Neurexin and Neuroligin Mediate Retrograde Synaptic Inhibition in *C. elegans*

Zhitao Hu^{1,2}, Sabrina Hom^{1,2,3}, Tambudzai Kudze¹, Xia-Jing Tong^{1,2}, Seungwon Choi^{1,2,3}, Gayane Aramuni⁴, Weiqi Zhang⁵, and Joshua M. Kaplan^{1,2,3,*}

¹Department of Molecular Biology, Massachusetts General Hospital, Boston, MA 02114, USA

²Department of Neurobiology, Harvard Medical School, Boston, MA 02115, USA

³Program in Neuroscience, Harvard Medical School

⁴Max Planck Institute of Neurobiology, D-82152 Martinsried, Germany

⁵Department of Psychiatry, University of Münster, D-48149 Münster, Germany

Abstract

The synaptic adhesion molecules Neurexin and Neuroligin alter the development and function of synapses and are linked to autism in humans. We find that *C. elegans* Neurexin (NRX-1) and Neuroligin (NLG-1) mediate a retrograde synaptic signal that inhibits neurotransmitter release at neuromuscular junctions. Retrograde signaling was induced in mutants lacking a muscle microRNA (miR-1) and was blocked in mutants lacking NLG-1 or NRX-1. Release was rapid and abbreviated when the retrograde signal was on whereas release was slow and prolonged when retrograde signaling was blocked. The retrograde signal adjusted release kinetics by inhibiting exocytosis of synaptic vesicles (SVs) that are distal to the site of calcium entry. Inhibition of release was mediated by increased pre-synaptic levels of Tomosyn, an inhibitor of SV fusion.

In *C. elegans*, a retrograde synaptic signal from muscle to motor neurons inhibits acetylcholine (ACh) release at neuromuscular junctions (NMJs) (1). This retrograde signal is induced by inactivation of a muscle microRNA (miR-1) and is abolished by inactivating the transcription factor MEF-2, a miR-1 target (1). In *mir-1* mutants, endogenous and evoked excitatory post-synaptic currents (EPSCs) recorded from body muscles were both diminished (Fig. 1), while synapse density is unaltered (1). Quantal content was significantly reduced in *mir-1* mutants, indicating decreased ACh release during evoked responses (Fig. 1E).

Because post-synaptic Neuroligin promotes maturation of pre-synapses and stimulates neurotransmitter release in mice (2–4), we tested the idea that *C. elegans* Neurexin (NRX-1) and Neuroligin (NLG-1) are required for the retrograde signal. Consistent with this idea, the endogenous and evoked EPSC defects observed in *mir-1* mutants were eliminated in *mir-1*; *nlg-1* and *mir-1*; *nrx-1* double mutants (Figs. 1 and S1). Retrograde inhibition of ACh release in *mir-1*; *nlg-1* double mutants was re-instated by transgenes expressing NLG-1 in

*Correspondence to: kaplan@molbio.mgh.harvard.edu.

Supplementary Materials:

www.sciencemag.org/cgi/content/full/science.XXXXXX

Materials and Methods

Figs. S1 to S8

References (25–28)

cholinergic motor neurons but not by those expressed in body muscles. Analogous rescue experiments suggested that NRX-1 functioned in body muscles (Fig. S1B, D).

The *nlg-1* promoter expressed GFP in cholinergic motor neurons but not in GABAergic neurons (Fig. S2A–B). When expressed in cholinergic DA and DB motor neurons, NLG-1::GFP exhibited a punctate distribution in dorsal cord axons but was diffuse in ventral cord dendrites (Fig. S2C). Dorsal cord NLG-1 puncta co-localized with a synaptic vesicle (SV) marker (mCherry-tagged UNC-57 endophilin) (Fig. S2C) (5). NRX-1::GFP expressed in body muscles was also punctate in the nerve cords and these NRX-1 puncta were often closely apposed to pre-synaptic UNC-57 puncta (Fig. S2D). Thus, NLG-1 and NRX-1 were pre- and post-synaptic respectively at cholinergic NMJs, opposite in polarity to their mammalian counterparts. Other examples of reversed polarity include presynaptic NLG-1 in worms (6, 7) and post-synaptic mouse and fly Neurexins (8–10).

If trans-synaptic adhesion mediates the retrograde signal, NRX-1 should bind directly to NLG-1. In transfected cells, we expressed a truncated NRX-1 containing the putative Neuroligin binding site (LNS6) (NRX-1[LNS6/HA]) and a soluble NLG-1 containing the entire extracellular domain fused to the IgG Fc domain (NLG-1/Fc) (Fig. S3). As expected, a significant fraction of NRX-1[LNS6/HA] bound to NLG-1/Fc when calcium was added but not when calcium was omitted (Fig. S3B, lanes 4–5). No binding was observed between Fc and NRX-1[LNS6/HA] (lanes 2–3).

Next, we analyzed *nlg-1* and *nrx-1* mutants for altered synapse development. Cholinergic NMJs were visualized with GFP-tagged pre- (SNB-1 synaptobrevin) and post-synaptic (ACR-16 ACh receptors) markers (Fig. S4). The fluorescent intensity and density of pre- and post-synaptic puncta were unaltered in *nlg-1* and *nrx-1* mutants. The rate and amplitude of endogenous EPSCs were also unchanged in *nlg-1* and *nrx-1* mutants (Figs. 1B and S1B). Therefore, inactivation of NLG-1 and NRX-1 did not grossly alter the morphology or formation of cholinergic NMJs.

If NRX-1 mediates the retrograde signal, its expression or function should be altered in *mir-1* mutants. Consistent with this idea, the fluorescent intensity of postsynaptic NRX-1 puncta was increased in *mir-1* mutants (40% increase, $p < 0.001$) and this effect was eliminated in *mir-1 mef-2* double mutants (Fig. 1F–H), where retrograde signaling is abolished (1). Thus, inducing the retrograde signal increased postsynaptic NRX-1 levels, consistent with NRX-1 acting downstream of miR-1 in this pathway. The NRX-1::GFP construct contains a promoter (*myo-3*) and 3'UTR (*unc-54*) that are not regulated by miR-1 (1); consequently, the effects of miR-1 and MEF-2 on NRX-1 expression are likely mediated by an indirect mechanism.

How does the retrograde signal alter ACh release? Evoked responses in *mir-1* mutants had decreased amplitude (Fig. 1E), faster decay (Fig. 2A–B), and faster charge transfer (Fig. 2C–D). To determine if these effects were caused by intrinsically faster muscle ACh responses, we analyzed endogenous EPSCs, which correspond to responses evoked by one SV fusion (11). As endogenous EPSC kinetics were unaltered in *mir-1* mutants (Fig. S5), the smaller evoked responses in *mir-1* mutants most likely resulted from faster and more abbreviated ACh release.

By contrast, quantal content was significantly increased when the retrograde was inactivated (in *nrx-1* and *nlg-1* mutants) (Figs. 1E and S1D) but was not further increased in *nrx-1; nlg-1* double mutants (*nlg-1* $n=13$, 872.1 ± 109.3 ; *nrx-1; nlg-1* $n=6$, 712.7 ± 53 , $p = 0.32$), consistent with NLG-1 and NRX-1 functioning together in this process. In *nlg-1* mutants, evoked responses exhibited slower decay and slower charge transfer, which were rescued by transgenes expressing NLG-1 in motor neurons (Figs. 2A–D and S6J). Endogenous EPSC

kinetics were unaltered in *nlg-1* mutants (Fig. S5). Consequently, the larger evoked responses in *nlg-1* mutants most likely resulted from slower and more prolonged ACh release. We could not analyze release kinetics in *nrx-1* mutants due to their faster quantal responses (Fig. S5), which confounds this analysis. The effects of miR-1 on evoked EPSC decay and charge transfer kinetics were eliminated in *mir-1; nlg-1* (Fig. 2E–H), *mir-1; nrx-1* (Fig. S6E–H), and *mir-1 mef-2* (Fig. S7) double mutants. Collectively, these results indicate that MEF-2, NRX-1, and NLG-1 all act downstream of miR-1 to mediate retrograde regulation of release kinetics.

Synaptic transmission was analyzed in mouse triple knockouts lacking NL1, NL2, and NL3 (3); however, the kinetics of evoked responses were not analyzed (3). When these data were re-analyzed, evoked EPSCs decayed significantly more slowly in NL1/2/3 triple knockouts than in single and double knockout controls (Fig. S8). The slower decay in triple knockouts likely resulted from a presynaptic change as mEPSC decay kinetics were unaltered. The kinetics of evoked and spontaneous IPSCs were not significantly altered in the NL1/2/3 triple knockouts (Fig. S8), indicating that this effect may be specific for glutamatergic synapses. Prolonged post-synaptic responses are also observed in mice expressing an autism associated NL3 allele (R451C) and in NL4 knockouts (12, 13). Thus, Neuroligins shape evoked response kinetics at worm and mouse synapses and can induce this effect from either a pre- or post-synaptic location.

How does the retrograde signal regulate release kinetics? SVs that are closer to calcium channels are expected to fuse more rapidly; consequently, the retrograde signal could adjust release kinetics by altering the ratio of proximal and distal SV fusions. To test this idea, we analyzed the effect of EGTA on EPSC kinetics. Because it binds calcium slowly, EGTA has little effect on fusion of SVs that are adjacent to calcium channels but potently inhibits fusion of SVs that are distal (or loosely coupled) to calcium channels (14). In wild type animals treated with membrane permeant EGTA (40 μ M EGTA-AM), evoked responses had decreased amplitude and quantal content and faster decay, all consistent with decreased fusion of distal SVs (Fig. 3). After EGTA-AM treatment, the quantal content, EPSC decay, and evoked current amplitude observed in wild type, *mir-1* and *nlg-1* mutants were very similar (Fig. 3). Thus, EGTA-AM eliminated the effects of miR-1 and NLG-1 on release, indicating that the retrograde signal inhibits ACh release and accelerates release kinetics by inhibiting fusion of distal SVs.

The retrograde signal could inhibit release by altering the distribution of pre-synaptic molecules that regulate SV fusion. The synaptic abundance of two active zone proteins (SYD-2/ Liprin and UNC-10/RIM) is unaffected in *mir-1* mutants (1). To further investigate this idea, we analyzed a third presynaptic protein, TOM-1/Tomosyn. In *tom-1* mutants, ACh release is increased, evoked EPSCs decay slowly, and there is a corresponding increase in the docking of SVs that are distal to dense projections (15, 16). Therefore, like the retrograde signal, TOM-1 inhibits fusion of distal SVs.

We analyzed the synaptic abundance of GFP-tagged TOM-1, which is co-localized with SVs at pre-synaptic terminals (15). TOM-1 puncta fluorescence was modestly increased in *mir-1* mutants (15% increase, $p < 0.05$) and this effect was eliminated in *mir-1; nlg-1* double mutants (Fig. 4A–B), indicating that the retrograde signal increased TOM-1 levels at pre-synapses. We next analyzed synaptic transmission in *tom-1 mir-1* double mutants. The effects of miR-1 on endogenous EPSC rate, quantal content, and evoked EPSC decay kinetics were eliminated in *tom-1 mir-1* double mutants (Fig. 4C–F). This double mutant analysis strongly supports the idea that TOM-1 acts downstream of miR-1. In *mir-1* single mutants, 64% of the EGTA sensitive component of evoked ACh release was eliminated (Fig. 3). If the *mir-1* mutation had a similar effect in *tom-1 mir-1* double mutants, quantal

content would be reduced by 48% whereas we observed a slight increase (6.2%, $p=0.67$) compared to *tom-1* single mutants. These results suggest that the retrograde signal bidirectionally adjusts the exocytosis rate of distal SVs and that it does so by regulating TOM-1.

Neurexin and Neuroligin mutations linked to autism spectrum disorders (ASD) and schizophrenia are proposed to alter cognition by perturbing synapse development (17). Our results support an additional mechanism whereby these mutations prolong post-synaptic responses. Mutations inactivating *nlx-1*, *nrx-1*, and *mef-2* in *C. elegans* were all associated with prolonged ACh release. Mutations in the corresponding human genes are all linked to ASD (18–20). Other ASD linked mutations alter post-synaptic response kinetics by other mechanisms, including altered expression of post-synaptic receptors (12, 13, 21) and altered clearance of secreted neurotransmitter (22).

Prolonged synaptic responses could have several important effects on circuit development and function. Prolonged responses would alter spike-timing dependent plasticity, and the temporal and spatial resolution of sensory responses. Functional imaging studies of ASD children indicate that acoustic responses are slower and that multisensory responses are integrated over a longer time window (23, 24), both consistent with slow and prolonged sensory responses. These results suggest that altered kinetics of synaptic responses could be an important cellular defect in ASD.

Supplementary Material

Refer to Web version on PubMed Central for supplementary material.

Acknowledgments

We thank the following for strains, advice, reagents, and comments on the manuscript: *C. elegans* stock center, S. Mitani, S. Sassi, B. Seed, and members of the Kaplan and Ruvkun labs. This work was supported by an NSF predoctoral fellowship (S.H.), and by research grants to J.K. from the NIH (NS32196) and from the Simons Foundation for Autism Research (SF177948). Additional data described in the manuscript are presented in the supporting online material.

References and Notes

1. Simon DJ, et al. The microRNA miR-1 regulates a MEF-2-dependent retrograde signal at neuromuscular junctions. *Cell*. 2008 May 30.133:903. [PubMed: 18510933]
2. Futai K, et al. Retrograde modulation of presynaptic release probability through signaling mediated by PSD-95-neuroligin. *Nat Neurosci*. 2007 Feb.10:186. [PubMed: 17237775]
3. Varoqueaux F, et al. Neuroligins determine synapse maturation and function. *Neuron*. 2006 Sep 21.51:741. [PubMed: 16982420]
4. Wittenmayer N, et al. Postsynaptic Neuroligin1 regulates presynaptic maturation. *Proc Natl Acad Sci U S A*. 2009 Aug 11.106:13564. [PubMed: 19628693]
5. Bai J, Hu Z, Dittman JS, Pym EC, Kaplan JM. Endophilin functions as a membrane-bending molecule and is delivered to endocytic zones by exocytosis. *Cell*. 2010 Oct 29.143:430. [PubMed: 21029864]
6. Hunter JW, et al. Neuroligin-deficient mutants of *C. elegans* have sensory processing deficits and are hypersensitive to oxidative stress and mercury toxicity. *Dis Model Mech*. 2010 May-Jun;3:366. [PubMed: 20083577]
7. Feinberg EH, et al. GFP Reconstitution Across Synaptic Partners (GRASP) defines cell contacts and synapses in living nervous systems. *Neuron*. 2008 Feb 7.57:353. [PubMed: 18255029]
8. Kattenstroth G, Tantalaki E, Sudhof TC, Gottmann K, Missler M. Postsynaptic N-methyl-D-aspartate receptor function requires alpha-neurexins. *Proc Natl Acad Sci U S A*. 2004 Feb 24.101:2607. [PubMed: 14983056]

9. Taniguchi H, et al. Silencing of neuroligin function by postsynaptic neurexins. *J Neurosci*. 2007 Mar 14;27:2815. [PubMed: 17360903]
10. Chen K, et al. Neurexin in embryonic *Drosophila* neuromuscular junctions. *PLoS One*. 2010; 5:e11115. [PubMed: 20559439]
11. Liu Q, et al. Presynaptic ryanodine receptors are required for normal quantal size at the *Caenorhabditis elegans* neuromuscular junction. *J Neurosci*. 2005 Jul 20;25:6745. [PubMed: 16033884]
12. Etherton M, et al. Autism-linked neuroligin-3 R451C mutation differentially alters hippocampal and cortical synaptic function. *Proc Natl Acad Sci U S A*. 2011 Aug 1.
13. Hoon M, et al. Neuroligin-4 is localized to glycinergic postsynapses and regulates inhibition in the retina. *Proc Natl Acad Sci U S A*. 2011 Feb 15;108:3053. [PubMed: 21282647]
14. Atluri PP, Regehr WG. Determinants of the time course of facilitation at the granule cell to Purkinje cell synapse. *J Neurosci*. 1996 Sep 15;16:5661. [PubMed: 8795622]
15. McEwen JM, Madison JM, Dybbs M, Kaplan JM. Antagonistic Regulation of Synaptic Vesicle Priming by Tomosyn and UNC-13. *Neuron*. 2006 Aug 3;51:303. [PubMed: 16880125]
16. Gracheva EO, et al. Tomosyn inhibits synaptic vesicle priming in *Caenorhabditis elegans*. *PLoS Biol*. 2006 Jul;4:e261. [PubMed: 16895441]
17. Sudhof TC. Neuroligins and neurexins link synaptic function to cognitive disease. *Nature*. 2008 Oct 16;455:903. [PubMed: 18923512]
18. Jamain S, et al. Mutations of the X-linked genes encoding neuroligins NLGN3 and NLGN4 are associated with autism. *Nat Genet*. 2003 May;34:27. [PubMed: 12669065]
19. Novara F, et al. Refining the phenotype associated with MEF2C haploinsufficiency. *Clin Genet*. 2010 Nov;78:471. [PubMed: 20412115]
20. Neale BM, et al. Patterns and rates of exonic de novo mutations in autism spectrum disorders. *Nature*. 2012 Apr 4.
21. Welch JM, et al. Cortico-striatal synaptic defects and OCD-like behaviours in Sapap3-mutant mice. *Nature*. 2007 Aug 23;448:894. [PubMed: 17713528]
22. Arnold PD, Sicard T, Burroughs E, Richter MA, Kennedy JL. Glutamate transporter gene SLC1A1 associated with obsessive-compulsive disorder. *Arch Gen Psychiatry*. 2006 Jul;63:769. [PubMed: 16818866]
23. Roberts TP, et al. MEG detection of delayed auditory evoked responses in autism spectrum disorders: towards an imaging biomarker for autism. *Autism Res*. 2010 Feb;3:8. [PubMed: 20063319]
24. Foss-Feig JH, et al. An extended multisensory temporal binding window in autism spectrum disorders. *Exp Brain Res*. 2010 Jun;203:381. [PubMed: 20390256]
25. Brenner S. The genetics of *Caenorhabditis elegans*. *Genetics*. 1974; 77:71. [PubMed: 4366476]
26. Richmond JE, Jorgensen EM. One GABA and two acetylcholine receptors function at the *C. elegans* neuromuscular junction. *Nat Neurosci*. 1999; 2:791. [PubMed: 10461217]
27. Burbea M, Dreier L, Dittman JS, Grunwald ME, Kaplan JM. Ubiquitin and AP180 regulate the abundance of GLR-1 glutamate receptors at postsynaptic elements in *C. elegans*. *Neuron*. 2002 Jul 3;35:107. [PubMed: 12123612]
28. Boucard AA, Chubykin AA, Comoletti D, Taylor P, Sudhof TC. A splice code for trans-synaptic cell adhesion mediated by binding of neuroligin 1 to alpha- and beta-neurexins. *Neuron*. 2005 Oct 20;48:229. [PubMed: 16242404]

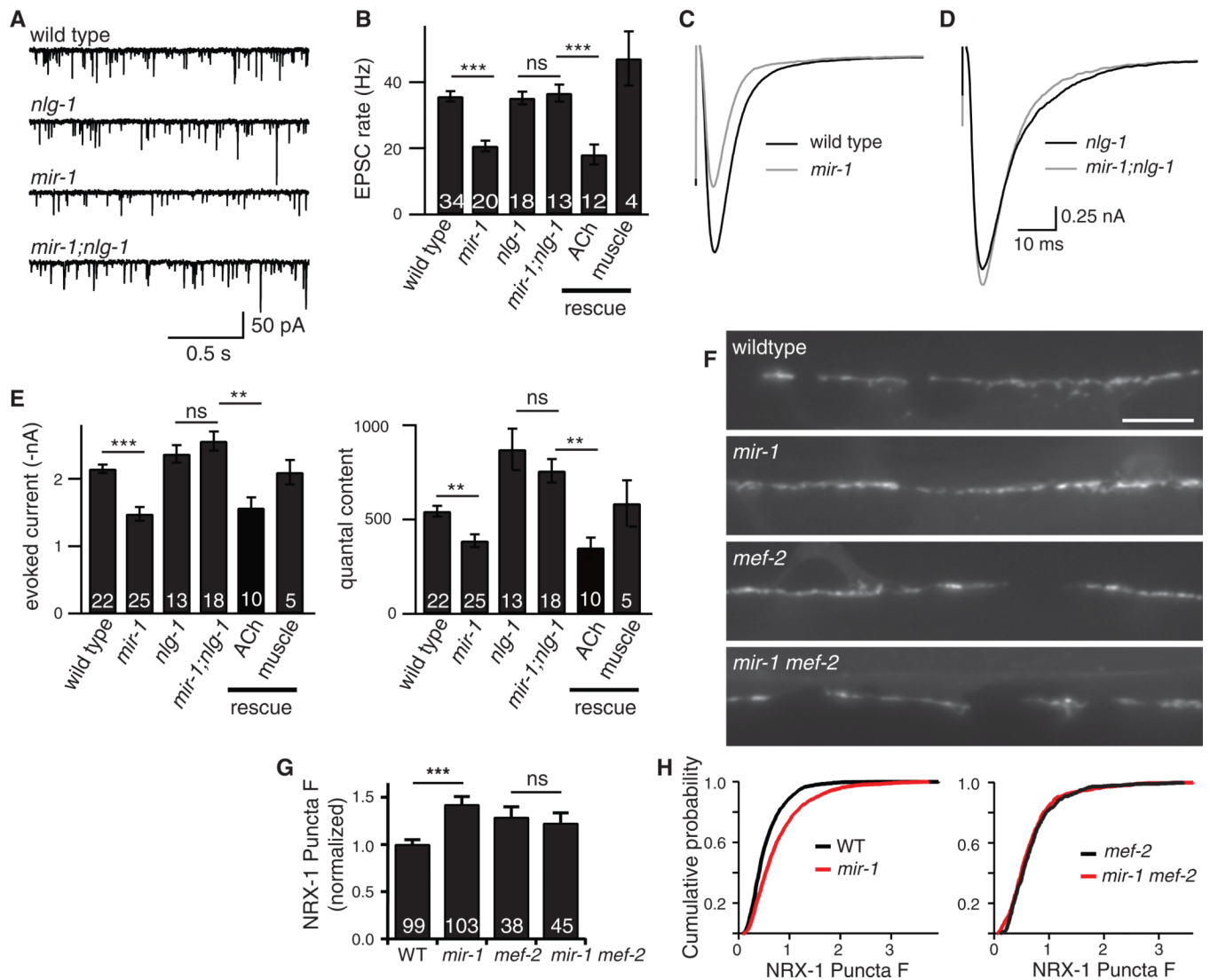


Figure 1. The retrograde signal was induced in *mir-1* mutants and inactivated in *nlg-1* mutants
Endogenous (A-B) and evoked EPSCs (C-E) were recorded from adult body wall muscles. Representative traces of endogenous EPSCs (A), averaged evoked responses (C-D), and summary data (B,E) are shown. The effects of miR-1 on EPSC rate and quantal content were eliminated in *mir-1; nlg-1* double mutants. (B,E) Retrograde inhibition was re-instated in *mir-1; nlg-1* double mutants by *nlg-1* transgenes expressed in cholinergic motor neurons (ACh rescue) but not by those expressed in body muscles (muscle rescue). (F-H) Expression of GFP-tagged NRX-1 in body muscles was analyzed. NRX-1 puncta fluorescence in the dorsal cord was significantly increased in *mir-1* mutants. This effect was eliminated in *mir-1 mef-2* double mutants. Representative images (F), mean (G), and cumulative probability distributions (H) of puncta intensity are shown. Values that differ significantly are indicated (***, $p < 0.001$; **, $p < 0.01$; ns, not significant). The number of animals analyzed is indicated for each genotype. Error bars indicate SEM. Scale bar indicates 5 μ m.

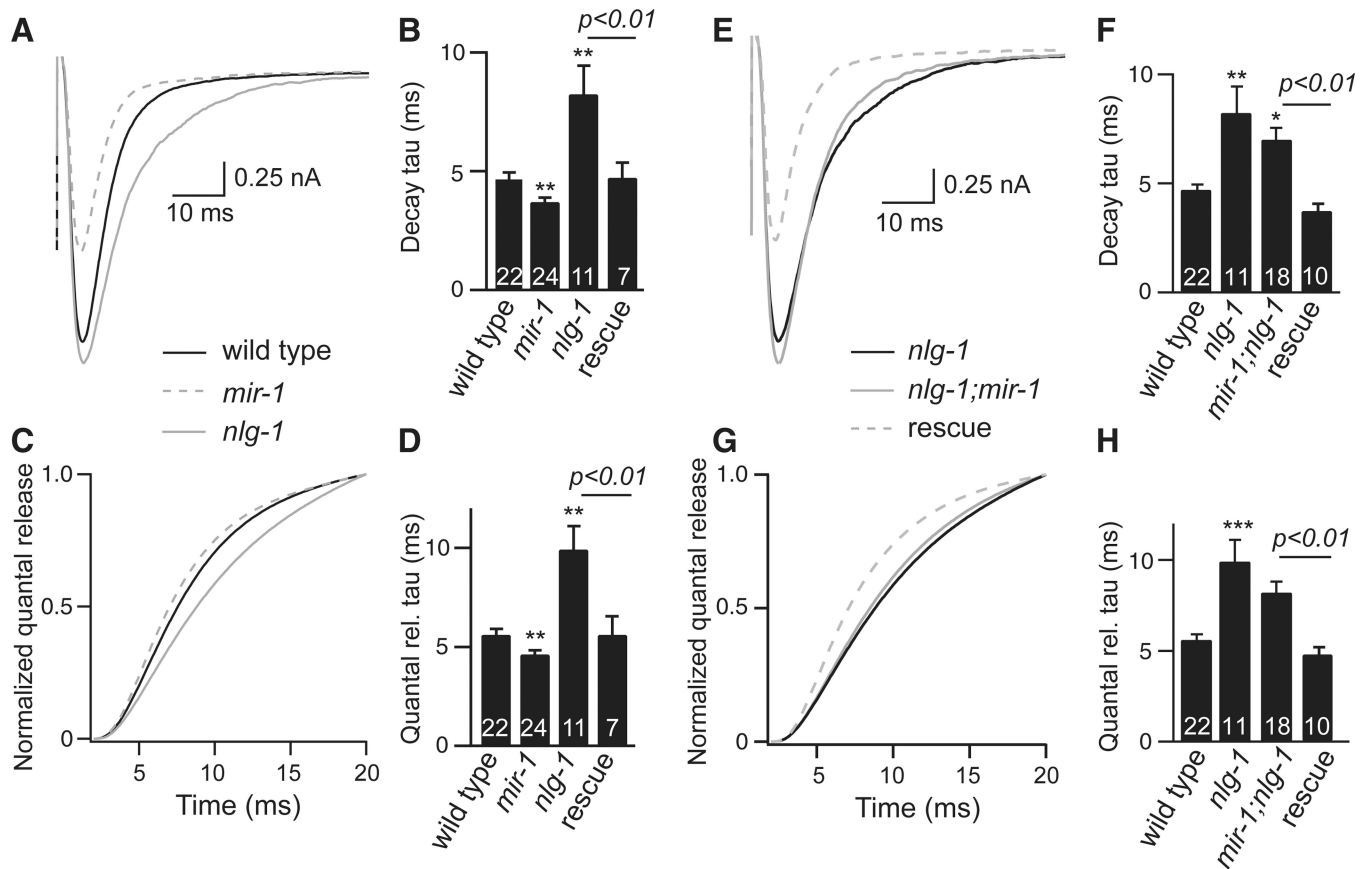


Figure 2. Activating and inactivating the retrograde signal had opposite effects on the kinetics of evoked responses

Evoked EPSCs were compared for the indicated genotypes. For each genotype, averaged evoked responses (A,E), decay kinetics (B,F), cumulative transfer of quantal charge (C,G), and charge transfer kinetics (D,H) are shown. Rescue refers to transgenic animals expressing NLG-1 in cholinergic neurons of *nlg-1* single mutants (B,D) and in *nlg-1; mir-1* double mutants (E-H). Values that differ significantly from wild type controls are indicated (***, $p < 0.001$; **, $p < 0.01$; *, $p < 0.05$). The number of animals analyzed is indicated for each genotype. Error bars indicate SEM.

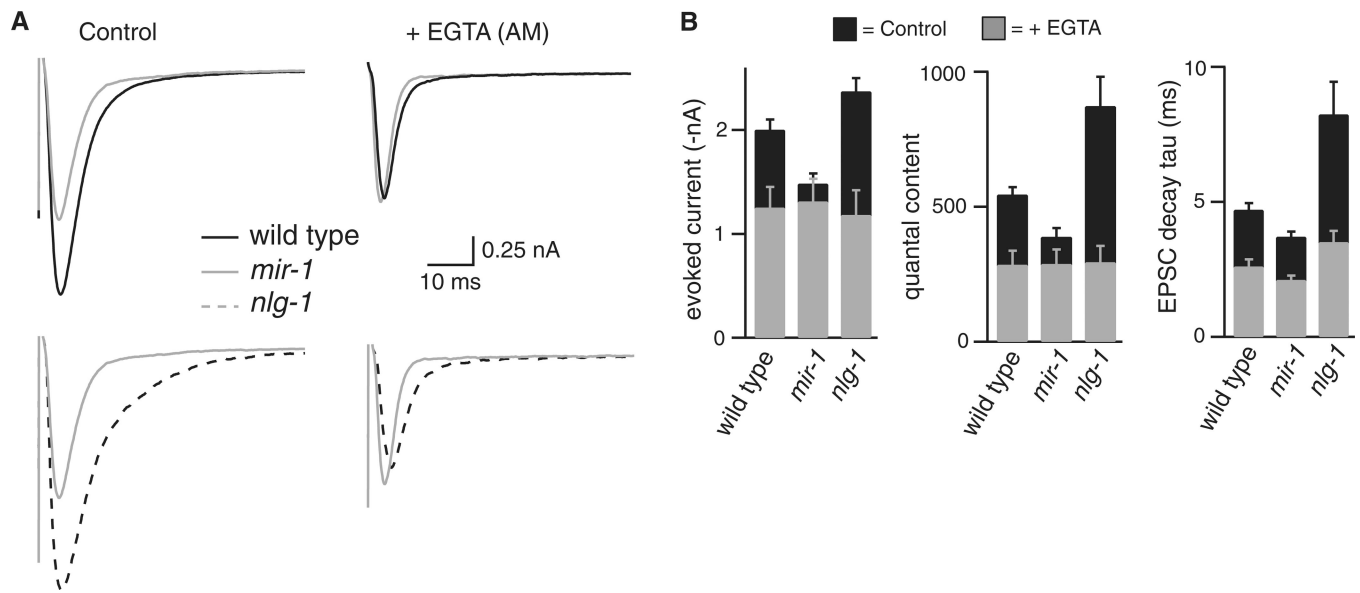


Figure 3. The effects of the retrograde signal on evoked responses are eliminated by EGTA
 (A) Averaged evoked responses are compared for wild type, *mir-1*, and *nlg-1* mutants with and without EGTA-AM treatment. (B) Summary data are shown comparing evoked EPSC amplitude, decay kinetics, and quantal content. The numbers of animals analyzed were: wild type (14 control, 12 + EGTA); *mir-1* (25 control, 11 + EGTA); and *nlg-1* (13 control, 8 + EGTA). Error bars indicate SEM. The amplitude, quantal content, and decay kinetics of evoked EPSCs were not significantly different in EGTA treated wild type, *mir-1*, and *nlg-1* animals: amplitude (WT vs. *mir-1*, $p = 0.976$; WT vs. *nlg-1*, $p = 0.972$); quantal content (WT vs. *mir-1*, $p = 0.999$; WT vs. *nlg-1*, $p = 0.993$); and decay tau (WT vs. *mir-1*, $p = 0.321$; WT vs. *nlg-1*, $p = 0.118$).

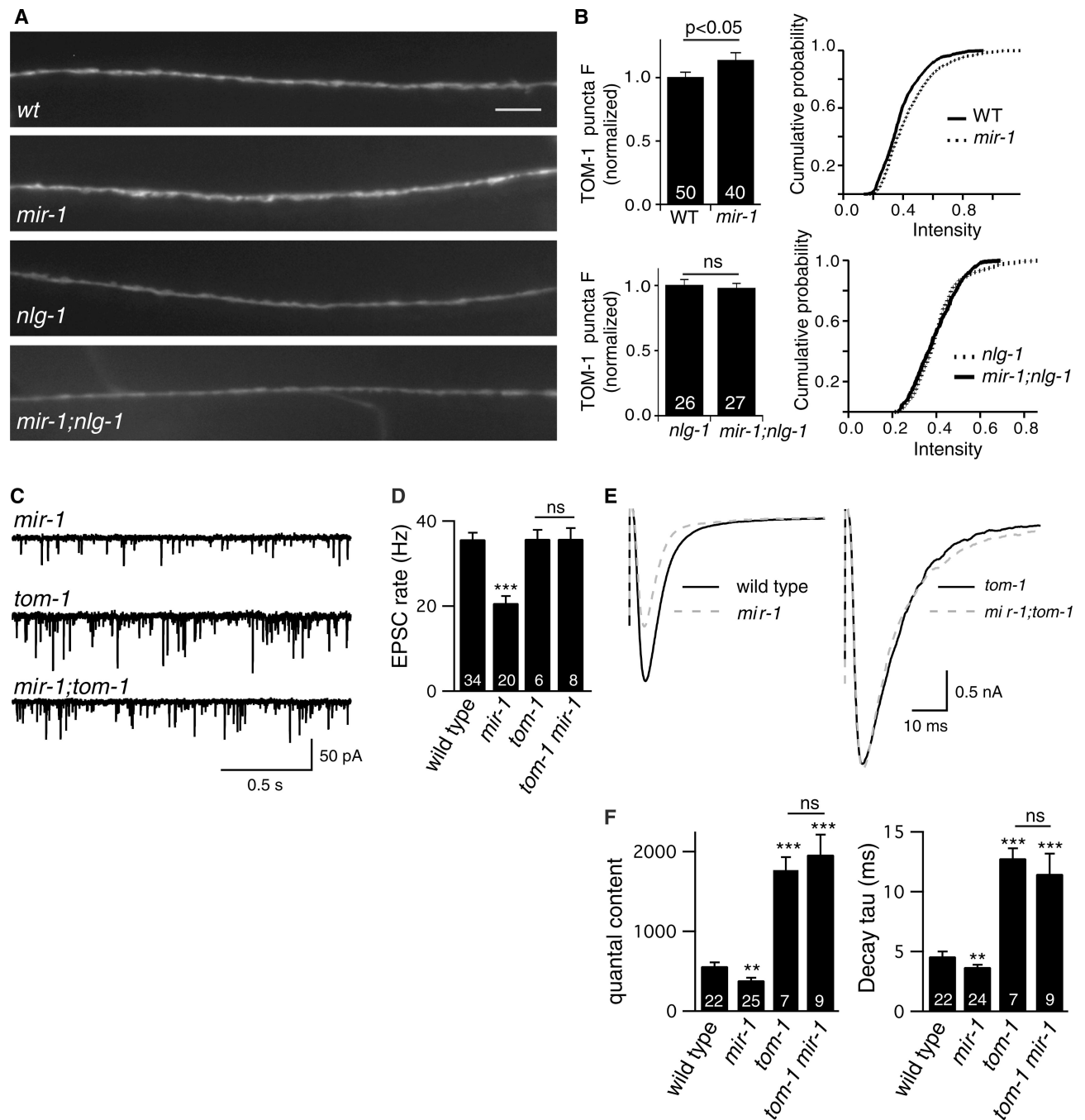


Figure 4. TOM-1/Tomosyn is required for the retrograde signal

(A-B) GFP-tagged TOM-1 was expressed in DA and DB motor neurons and puncta fluorescence was analyzed in the dorsal nerve cord. Representative images (A), mean and cumulative probability distributions of puncta intensity (B) are shown. TOM-1 puncta intensity was significantly increased in *mir-1* mutants. This effect was eliminated in *mir-1;nlg-1* double mutants. Scale bar indicates 5 μ m. (C-F) Endogenous (C-D) and evoked EPSCs (E-F) were recorded from adult body wall muscles. Representative traces of endogenous EPSCs (C), averaged evoked responses (E), and summary data (D,F) are shown. The effects of miR-1 on EPSC rate, quantal content, and evoked decay kinetics were eliminated in *tom-1 mir-1* double mutants. Values that differ significantly from wild type controls are

indicated (***, $p < 0.001$; **, $p < 0.01$; ns, not significant). The number of animals analyzed is indicated for each genotype. Error bars indicate SEM.